

Fast and accurate optimization on the orthogonal manifold without retraction

Pierre Ablin Gabriel Peyré

CNRS, Département de mathématiques et applications, ENS
PSL University

We consider the problem of minimizing a function over the manifold of orthogonal matrices. The majority of algorithms for this problem compute a direction in the tangent space, and then use a retraction to move in that direction while staying on the manifold. Unfortunately, the numerical computation of retractions on the orthogonal manifold always involves some expensive linear algebra operation, such as matrix inversion or matrix square-root. These operations quickly become expensive as the dimension of the matrices grows. To bypass this limitation, we propose the landing algorithm which does not involve retractions. The algorithm is not constrained to stay on the manifold but its evolution is driven by a potential energy which progressively attracts it towards the manifold. One iteration of the landing algorithm only involves matrix multiplications, which makes it cheap compared to its retraction counterparts. We provide an analysis of the convergence of the algorithm, and demonstrate its promises on large-scale problems, where it is faster and less prone to numerical errors than retraction-based methods.

1. Introduction

We consider a differentiable function f from $\mathbb{R}^{p \times p}$ to \mathbb{R} , and want to solve the problem

$$\min_{X \in \mathcal{O}_p} f(X) , \quad (1)$$

where \mathcal{O}_p is the *Orthogonal manifold*, that is the set of matrices $X \in \mathbb{R}^{p \times p}$ such that $XX^\top = I_p$. Problem (1) appears in many practical applications, like principal component analysis, independent component analysis (Comon, 1994; Nishimori, 1999; Ablin et al., 2018), procrustes problem (Schönemann, 1966), and more recently in deep learning, where the weights of a layer are parametrized by an orthogonal matrix (Arjovsky et al., 2016; Bansal et al., 2018). This is a particular instance of minimization over a matrix Riemannian manifold, \mathcal{O}_p (Edelman et al., 1998). Many standard Euclidean algorithms for function

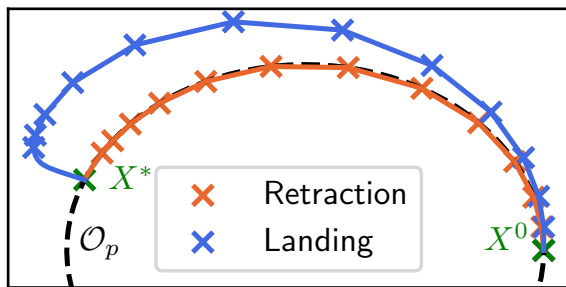


Figure 1: Trajectories of the landing algorithm and of a retraction gradient descent on an orthogonal Procrustes problem, with $p = 2$. The iterates are 2×2 matrices, we only display the behavior of the first column: the x -axis corresponds to coefficient $(1, 1)$ of the matrices, and the y -axis to coefficient $(1, 2)$. The retraction method stays on \mathcal{O}_p (black dotted line) while the landing algorithm moves away from the manifold. Both methods start from X_0 and converge to the correct solution X_* . In higher dimension, the retraction method is much more expensive than the landing algorithm.

minimization have been adapted on Riemannian manifolds. We can cite for instance gradient descent (Absil et al., 2009; Zhang & Sra, 2016), second order quasi-Newton methods (Absil et al., 2007; Qi et al., 2010), and stochastic methods (Bonnabel, 2013) which are the workhorse for training deep neural networks. More recently, several works propose to adapt accelerated methods in the Riemannian setting (Zhang & Sra, 2018; Tripuraneni et al., 2018).

All these methods are *feasible*, i.e. generate a sequence of iterates X_k where each iterate is in \mathcal{O}_p . Unlike what we assume in the first sentence of the present article, they do not need the function f to be defined outside \mathcal{O}_p . This comes with a computational drawback: in order to compute X_{k+1} from X_k , one needs a way to move and stay on the manifold, called *retraction* (Absil & Malick, 2012). Unfortunately, retractions on \mathcal{O}_p are computationally expensive: they typically require some matrix inversion, square root, or exponential. On top of being already expensive, these operations are generally slow on modern computing hardware like GPU's. Consequently, when the dimension p is large, computing the retraction can become the computational bottleneck in the processing pipeline.

In this work, we propose the **landing algorithm**. It is an *infeasible* method, which produces iterates X_k that are not necessarily orthogonal, but which converge to a local minimum of (1) as $k \rightarrow +\infty$. The iterates get closer and closer to the manifold, and at the limit, *land* on \mathcal{O}_p . The algorithm is illustrated in Figure 1 on a low dimensional problem. The main advantage of the method is that the update rule is much simpler than a retraction, as it only involves a few matrix multiplications. As a consequence, our method can be much faster than standard feasible methods when p is large.

Furthermore, retraction methods often suffer from an accumulation of numerical errors, which means that the iterates can get far from \mathcal{O}_p after many steps of the algorithm. This effect is worsened by the low precision of floating point number that is customary in

modern deep learning frameworks. On the other hand, our method can only converge to matrices such that $\|XX^\top - I_p\| = 0$ to numerical precision. Even though the proposed method is infeasible, it actually returns a solution that is closer to the manifold than most feasible methods in practice.

The article is organized as follows: in Section 2, we recall some usual results about the geometry of \mathcal{O}_p and Riemannian optimization algorithms. In Section 3, we introduce the landing algorithm, provide a convergence analysis, and discuss some possible extensions. Finally, we present numerical results in Section 4, which demonstrate the usefulness of replacing retraction methods by the landing algorithm in terms of computational efficiency and final distance to the orthogonal manifold.

Notation: Skew_p is the set of skew-symmetric matrices, Sym_p is the set of symmetric $p \times p$ matrices. The Skew of a matrix $M \in \mathbb{R}^{p \times p}$ is $\text{Skew}(M) = \frac{1}{2}(M - M^\top)$, and the Sym is $\text{Sym}(M) = \frac{1}{2}(M + M^\top)$. The Euclidean gradient of f is ∇f , the Riemannian gradient is $\text{Grad } f$. The matrix norm is the Frobenius ℓ^2 norm. The squared “distance” to the manifold is $\mathcal{N}(X) = \frac{1}{2}\|XX^\top - I_p\|^2$.

We give sketches of proof for propositions in the main text. Detailed proofs are deferred to the appendix.

2. Preliminaries

In this section, we recall basic concepts about optimization on manifolds that will be useful in the rest of this article.

2.1. Geometry of the orthogonal manifold

The orthogonal manifold is $\mathcal{O}_p \triangleq \{X \in \mathbb{R}^{p \times p} \mid XX^\top = I_p\}$. If $X(t)$ for $t \in [0, 1]$ is a differentiable curve on the manifold, differentiating the equation $X(t)X(t)^\top = I_p$ gives $\dot{X}(t)X(t)^\top + X(t)\dot{X}(t)^\top = 0$, hence $\dot{X}(t) \in \mathcal{T}_{X(t)}$ where \mathcal{T}_X is the *tangent space* at X , given by $\mathcal{T}_X = \{\xi \in \mathbb{R}^{p \times p} \mid \xi X^\top + X\xi^\top = 0\}$.

We see that a matrix ξ is in \mathcal{T}_X if and only if for some skew-symmetric matrix A we have $\xi = AX$. It then easily seen that the tangent space is a linear space of dimension $\frac{p(p-1)}{2}$. The tangent space is equipped with the canonical scalar product. We will finally need the projection on the manifold $\mathcal{P}(X) \triangleq \arg \min_{Y \in \mathcal{O}_p} \|X - Y\|$, which is $\mathcal{P}(X) = (XX^\top)^{-\frac{1}{2}}X$, defined for any invertible X . We now turn our attention to optimization on \mathcal{O}_p .

2.2. Relative optimization on \mathcal{O}_p and extension to $\mathbb{R}^{p \times p}$

Vectors in the tangent space at X are of the form AX with $A \in \text{Skew}_p$. The effect of small perturbations of X in the direction AX on f leads to so-called *relative* derivatives (Cardoso & Laheld, 1996):

Definition 1. For $X \in \mathbb{R}^{p \times p}$, the relative gradient $\psi(X) \in \text{Skew}_p$ is defined with the Taylor expansion, for $A \in \text{Skew}_p$:

$$f(X + AX) = f(X) + \langle A, \psi(X) \rangle + o(\|A\|). \quad (2)$$

The relative Hessian \mathcal{H}_X is the linear operator $\text{Skew}_p \rightarrow \text{Skew}_p$ such that

$$\psi(X + AX) = \psi(X) + \mathcal{H}_X(A) + o(\|A\|). \quad (3)$$

These quantities are not defined only on \mathcal{O}_p , but on the whole $\mathbb{R}^{p \times p}$, and can be computed easily from the Euclidean derivatives of f . The projection on the skew-symmetric matrices, defined as $\text{Skew}(M) = \frac{1}{2}(M - M^\top)$ plays an important role here.

Proposition 1 (Relative gradient from Euclidean gradient). *Let $\nabla f(X) \in \mathbb{R}^{p \times p}$ the Euclidean gradient and $H_X : \mathbb{R}^{p \times p} \rightarrow \mathbb{R}^{p \times p}$ the Euclidean Hessian of f at X . We have*

$$\begin{aligned} \psi(X) &= \text{Skew}(\nabla f(X)X^\top) \quad \text{and} \\ \mathcal{H}_X(A) &= \text{Skew}(H_X(AX)X^\top - \nabla f(X)X^\top A) \end{aligned}$$

We can recover the Riemannian gradient and Hessian of f from the Relative derivatives:

Proposition 2 (Riemannian derivatives from relative derivatives). *For $X \in \mathcal{O}_p$, we have $\text{Grad } f(X) = \psi(X)X$, and for $A \in \text{Skew}_p$, we have $\text{Hess } f(X)(AX) = \mathcal{H}_X(A)X + \text{Skew}(\psi(X)A)X$.*

Proof. The Riemannian gradient of f is such for $\xi \in \mathcal{T}_X$, it holds $f(X + \xi) = f(X) + \langle \text{Grad } f(X), \xi \rangle + o(\|\xi\|)$. Letting $A = \xi X^\top \in \text{Skew}_p$, we find $\langle \text{Grad } f(X), \xi \rangle = \langle \psi(X), A \rangle = \langle \psi(X)X, \xi \rangle$ which shows $\text{Grad } f(X) = \psi(X)X$. Further, the Riemannian Hessian is given by $\text{Hess } f(X)(\xi) = \text{Skew}(H_X(\xi)X^\top - \text{Sym}(\nabla f(X)X^\top) \xi X^\top) X$ (Absil et al., 2013, Sec. 4.3), which concludes the proof. \square

Therefore, the critical points of f on \mathcal{O}_p , i.e. the points such that $\text{Grad } f(X) = 0$, are exactly the points such that $\psi(X) = 0$, and at those points, we have $\text{Hess } f(X)(AX) = \mathcal{H}_X(A)X$: the Hessians are the same up to a remapping, and therefore share the same spectrum.

2.3. Optimization on the orthogonal manifold with retractions

A simple method to solve Problem (1) is the Riemannian gradient flow, which is the Ordinary Differential Equation (ODE) starting from $X_0 \in \mathcal{O}_p$

$$X(0) = X_0, \quad \dot{X}(t) = -\text{Grad } f(X(t)) . \quad (4)$$

It is easily seen that the trajectory of the ODE stays in \mathcal{O}_p , and that $f(X(t))$ decreases with t . Further assumptions on f , like Polyak-Lojasiewicz inequalities (Karimi et al., 2016; Balashov et al., 2020) or geodesic strong-convexity allow to prove the convergence of $X(t)$ to a minimizer as $t \rightarrow +\infty$. In order to obtain a practical optimization algorithm, one should discretize the gradient flow. Sadly, a naive Euler discretization, which iterates $X_{k+1} = X_k - \eta \text{Grad } f(X_k)$ with $\eta > 0$ gives iterates that do not belong to the manifold, because the curvature is not taken into account.

This motivates the use of retractions. A retraction \mathcal{R} maps (X, ξ) where $X \in \mathcal{O}_p$ and $\xi \in \mathcal{T}_X$ to a point $\mathcal{R}(X, \xi) \in \mathcal{O}_p$, and is such that $\mathcal{R}(X, \xi) = X + \xi + o(\|\xi\|)$. Since the tangent space has such a simple structure, it is easier to describe a retraction with the mapping $\tilde{\mathcal{R}}(X, A)$, where $A \in \text{Skew}_p$, such that $\tilde{\mathcal{R}}(X, A) = \mathcal{R}(X, AX)$. The following table lists three popular retractions.

Name	Formula
Exponential	$\tilde{\mathcal{R}}(X, A) = \exp(A)X$
Projection	$\tilde{\mathcal{R}}(X, A) = \mathcal{P}(X + AX)$
Cayley	$\tilde{\mathcal{R}}(X, A) = (I_p - \frac{A}{2})^{-1}(I_p + \frac{A}{2})X$

These retractions all involve linear algebra operations on matrices like inversion, square root, or exponential. We show that there is no “simpler” retraction:

Proposition 3 (No polynomial retraction). *There is no $P(X, A)$ polynomial in the two variables such that $\tilde{\mathcal{R}}(X, A) = P(X, A)$ is a retraction.*

Proof. By contradiction, such polynomial must satisfy $P(X, A)P(X, A)^\top = I_p$. This implies that the degree of PP^\top is 0, hence P is of degree 0, and P is constant. Therefore, we cannot have $P(X, A) = X + AX + o(\|AX\|)$. \square

As a consequence, *any* retraction must involve some linear algebra more complicated than matrix multiplication.

Riemannian gradient descent uses a retraction to stay on the manifold. It iterates

$$X_{k+1} = \mathcal{R}(X_k, -\eta \text{Grad } f(X_k)) , \quad (5)$$

where $\eta > 0$ is a step-size. Riemannian gradient descent is conveniently written with the relative gradient ψ as $X_{k+1} = \tilde{\mathcal{R}}(X_k, -\eta\psi(X_k))$. We now present the landing algorithm, which *does not require retractions*.

3. The landing algorithm

In the following, we make use of the function $\mathcal{N}(X) \triangleq \frac{1}{2}\|XX^\top - I_p\|^2$. This function vanishes if and only if $X \in \mathcal{O}_p$. A simple way to build an algorithm that converges to \mathcal{O}_p consists in following $-\nabla\mathcal{N}(X)$, which leads in the continuous setting to Oja’s flow $\dot{X} = -\nabla\mathcal{N}(X)$ (Oja, 1982; Yan et al., 1994) and in the discrete setting to Potter’s algorithm $X_{k+1} = X_k - \eta\nabla\mathcal{N}(X_k)$ (Cardoso & Laheld, 1996). Note that the Euclidean gradient has the simple formula $\nabla\mathcal{N}(X) = (XX^\top - I_p)X$, and that it is always orthogonal to the Riemannian gradient of f , since $\nabla\mathcal{N}(X)$ is written as SX with $S \in \text{Sym}_p$, while $\text{Grad } f(X)$ is written as AX with $A \in \text{Skew}_p$.

The landing algorithm combines the previous orthogonalizing method with the minimization of f . We define the **landing field** as the mapping $\mathbb{R}^{p \times p} \rightarrow \mathbb{R}^{p \times p}$:

$$\boxed{\Lambda(X) \triangleq \psi(X)X + \lambda\nabla\mathcal{N}(X)} , \quad (6)$$

where $\lambda > 0$ is a fixed parameter. This allows to define the **landing algorithm**, which iterates:

$$X_{k+1} = X_k - \eta^k \Lambda(X_k) , \quad (7)$$

with $\eta^k > 0$ a sequence of step-sizes. Its continuous counterpart is the **landing flow**:

$$\dot{X}(t) = -\Lambda(X(t)). \quad (8)$$

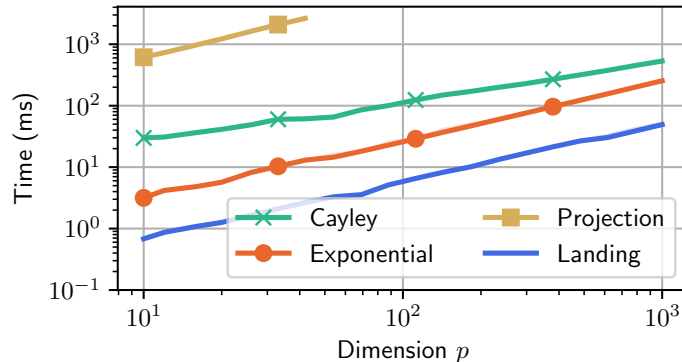


Figure 2: Time required to compute a retraction $\tilde{\mathcal{R}}(X, A)$ when A and X are given matrices of size $p \times p$, for the most popular retractions. Computing the landing field (Eq. (6)) is much cheaper.

We stress that the field Λ is not the Riemannian gradient nor the Euclidean gradient of a function. In particular, the landing flow does *not* have the same trajectory as the Euclidean gradient flow associated to the function $f(X) + \lambda\mathcal{N}(X)$.

Before we move on to the analysis of the algorithm, we can already see that one iteration of the landing algorithm only involves some matrix multiplications instead of expensive linear algebra. In Figure 2, we show the cost of computing on a GPU one iteration of the Riemannian gradient descent using the standard retractions, and the cost of computing one iteration of the landing algorithm as p grows. The proposed method is about 4 times faster than retraction methods.

Computational cost of Riemannian gradient descent Riemannian gradient descent on \mathcal{O}_p first computes the descent direction, using the Euclidean gradient of f , and then computes the next iterate using a retraction. Depending on the problem, the main computational bottleneck can come from either steps. For instance, when training a Recurrent Neural Network (RNN) with orthogonal weights (Arjovsky et al., 2016; Lezcano Casado, 2019), there is usually only one orthogonal matrix which is used in a large computational graph. Here, the cost of computing the Euclidean gradient with backpropagation is much larger than that of computing a retraction. As a consequence, using the landing algorithm in this setting will only marginally reduce the cost of computations. On the other hand, it is common to impose an orthogonality constraint on multi-layer perceptron or on convolutional neural networks (Rodríguez et al., 2016; Bansal et al., 2018). This constraint has been reported to give faster training and better generalization. In this case, there are many orthogonal matrices, and the main bottleneck of training can be the computation of the retraction. As we will see in the experiments, it is thus interesting to use the landing algorithm in this setting.

We now turn to a theoretical analysis of the method, and begin by a study of the critical points.

Proposition 4 (Critical points of Λ). *Let $X \in \mathbb{R}^{p \times p}$ invertible. We have $\Lambda(X) = 0$ if and only if $X \in \mathcal{O}_p$ and $\psi(X) = 0$.*

Proof. If $\Lambda(X) = 0$, we have $\psi(X) + \lambda(XX^\top - I_p) = 0$. By projection on the symmetric matrices, the previous result yields $XX^\top = I_p$, i.e. $X \in \mathcal{O}_p$. By projection on the skew-symmetric matrices, we find $\psi(X) = 0$. Conversely, if $\psi(X) = 0$ and $X \in \mathcal{O}_p$, we have $\Lambda(X) = 0$ \square

This result shows that the stationary points of the landing algorithm are the stationary points of the original problem (1). It holds regardless of the value of the hyper-parameters λ .

3.1. Orthogonalization property

We start by showing that the landing flow (8) is *orthogonalizing*: the flow converges to the orthogonal manifold.

Proposition 5 (Convergence of the flow to \mathcal{O}_p). *Let $X(t)$ the solution of the landing flow (8). Then, $\mathcal{N}(X(t))$ decreases, and denoting $N_0 \triangleq \mathcal{N}(X_0)$, we have $\mathcal{N}(X(t)) \leq e^{-\lambda t} \left(\frac{N_0}{(\sqrt{N_0}-1)^2} \right)$.*

Proof. Let $n(t) = \mathcal{N}(X(t))$. We find $n'(t) = \langle \dot{X}(t), \nabla \mathcal{N}(X(t)) \rangle$. Then, we have for all X , $\langle \psi(X)X, \nabla \mathcal{N}(X) \rangle = \langle \psi(X), (XX^\top - I_p)XX^\top \rangle$. The matrix on the left is skew-symmetric, the matrix on the right is symmetric, hence this scalar product cancels. Therefore, we get $n'(t) = -\|\nabla \mathcal{N}(X(t))\|^2$. This shows that $n(t)$ decreases. Next, we use the inequality $\|(XX^\top - I_p)X\|^2 \geq \mathcal{N}(X) - \mathcal{N}(X)^{\frac{3}{2}}$ which allows us to conclude. \square

This shows that the landing flow produces a trajectory that *lands* on the manifold: the distance to the manifold decreases, and goes to 0 at a linear rate. As a corollary, if the landing flow starts on the manifold ($X_0 \in \mathcal{O}_p$), then $\mathcal{N}(X(t)) = 0$ for all $t \geq 0$, i.e. the flow stays on the manifold, and is equal to the Riemannian gradient flow (4).

3.2. Safe rule for the discrete algorithm

Things are more complicated in the discrete case. For instance if $X_0 \in \mathcal{O}_p$, then $X_1 = X_0 - \eta\psi(X_0)X_0$ is never orthogonal. Therefore, there is no hope that $\mathcal{N}(X_k)$ is a decreasing sequence. Instead, we set $\varepsilon > 0$, and get a criterion on the step-size which ensures $\mathcal{N}(X_k) \leq \varepsilon$ for all k .

Proposition 6 (Safe step-size interval). *Assume that X_k is such that $d \triangleq \mathcal{N}(X_k) \leq \varepsilon$. Let $a \triangleq \|\psi(X_k)\|$ and $\eta^*(a, d) \triangleq \frac{\sqrt{\alpha^2 + 4\beta(\varepsilon-d)} + \alpha}{2\beta}$, where $\alpha \triangleq 2\lambda d - 2ad - 2\lambda d^2$ and $\beta \triangleq a^2 + \lambda^2 d^3 + 2\lambda ad^2 + a^2 d$. Then if $\eta \in [0, \eta^*(a, d)]$, we have $\mathcal{N}(X_{k+1}) \leq \varepsilon$.*

As a consequence, if the algorithm starts from $X_0 \in \mathcal{O}_p$ and η is in the safe interval for each step, the iterates all verify $\mathcal{N}(X_k) \leq \varepsilon$. It is worth mentioning that while the above formula is complicated, it is only a matter of computing a scalar function given $\|\phi(X_k)\|$ and $\mathcal{N}(X_k)$, so computing $\eta^*(a, d)$ is negligible in front of the other computations. In practice, we provide a sequence of target step-size η_k to the algorithm, and at each iteration, we compute η^* . We then use $\min(\eta_k, \eta^*)$ as the step-size. Importantly, we see

that when $a = 0$, the safe step-size is of the order $\eta^* \simeq \frac{4}{\lambda d^2} \leq \frac{4}{\lambda \varepsilon^2}$, which is typically a large number when ε is small. This safe rule therefore does not restrict much the choice of step-size, which is also observed in practice. This allows us to give a safe landing algorithm, which is given in Algorithm 1.

Algorithm 1 Landing algorithm with safe step-size

Input : Initial point $X_0 \in \mathcal{O}_p$, step-size sequence η_k , number of iterations N .
for $k = 1$ **to** N **do**
 Compute η^* (Proposition 6)
 Set $\eta_k = \min(\eta^*, \eta_k)$
 Update $X_{k+1} = X_k - \eta_k \Lambda(X_k)$
end for
Return : X_N .

We now study the convergence of the landing algorithm towards \mathcal{O}_p . Since the orthogonalization error and the relative gradient $\psi(X_k)$ are intertwined, we do not provide a proof of convergence in the general case. We rather view $\psi(X_k)$ as a perturbation quantity that goes to 0. We consider two settings: one where convergence is linear, e.g. $\|\psi(X_k)\| \simeq \omega^k$ for some $\omega < 1$, and one where convergence is sub-linear, e.g. $\|\psi(X_k)\| \simeq k^\alpha$ for some $\alpha < 0$.

Proposition 7 (Linear convergence of the algorithm to \mathcal{O}_p). *Assume that the sequence $a_k = \|\psi(X_k)\|$ satisfies $a_k = O(\omega^k)$ for some $\omega \in (0, 1)$, and that the step-size is fixed to $\eta \leq \frac{1}{2\lambda}$. For any $\delta > 0$, we have $\mathcal{N}(X_k) = O((\max(1 - 2\eta\lambda, \omega) + \delta)^k)$.*

Proof. We show that for k large enough $\mathcal{N}(X_k)$ satisfies a recursion of the form $\mathcal{N}(X_{k+1}) \leq (1 - 2\eta\lambda + \delta)\mathcal{N}(X_k) + C(\omega + \delta)^k$, where C is a constant. Unrolling the recursion gives the advertised rate of convergence. \square

Proposition 8 (Sublinear convergence of the algorithm to \mathcal{O}_p). *Assume that the sequence $a_k = \|\psi(X_k)\|$ satisfies $a_k = O(k^\alpha)$ for some $\alpha < 0$, and that the step-size is fixed to $\eta \leq \frac{1}{2\lambda}$. For any $\delta > 0$, we have $\mathcal{N}(X_k) = O(k^{\alpha+\delta})$.*

Proof. Similarly, we show that for k large enough, it holds $\mathcal{N}(X_{k+1}) \leq (1 - 2\eta\lambda + \delta)\mathcal{N}(X_k) + Ck^{\alpha+\delta}$. Unrolling the recursion provides the correct rate. \square

These propositions show that d_k goes to 0, at the slowest rate between the rate of convergence of the minimization of f , and the rate of convergence of the orthogonalization algorithm when $\psi = 0$. This behavior is observed in practice.

Stochastic method and distance to \mathcal{O}_p in the small gradient regime When f has a sum structure: $f(X) = \sum_{i=1}^n f_i(X)$, it is possible to use stochastic gradient descent, which takes a step in the opposite direction of the gradient of one of the f_i instead of f . Such method is easily adapted to the Riemannian setting, by taking Riemannian stochastic gradients and using retractions, or the landing algorithm. If we let ψ_i the relative gradient of the function f_i , the stochastic landing algorithm samples i_k at random between 1 and Q , and then does a step $X_{k+1} = X_k - \eta_k (\psi_{i_k}(X_k) + \lambda(X_k X_k^\top - I_p)) X_k$.

We give an informal computation to control the distance of the iterates to \mathcal{O}_p when the gradients $\psi_i(X_k)$ are small. Denoting $\Delta_k \triangleq X_k X_k^\top - I_p$, and neglecting high order terms in ψ and Δ_k , one has the approximate relationship

$$\Delta_{k+1} \simeq (1 - 2\eta_k \lambda) \Delta_k - \eta_k^2 (\psi_i(X_k))^2. \quad (9)$$

Assuming that the gradients $\psi_i(X_k)$ are independent from Δ_k and have an average norm a , we find

$$\mathbb{E}[\|\Delta_{k+1}\|^2] = (1 - 2\eta_k \lambda)^2 \mathbb{E}[\|\Delta_k\|^2] + \eta_k^4 a^4.$$

If the step-sizes η_k are fixed to $\eta > 0$, the above equation indicates that $\mathbb{E}[\|\Delta_k\|^2]$ converges to a limit value given by

$$(\mathbb{E}[\|\Delta_k\|^2])^{1/2} \rightarrow \delta_* \triangleq \frac{\eta a^2}{2\lambda}. \quad (10)$$

The above reasoning is informal and there are many approximations. However, in the practical experiments with stochastic algorithms, we find that δ^* is close to the distance to the manifold \mathcal{O}_p observed in practice. We now turn to a convergence analysis.

3.3. Local convergence

In this section, we assume that the iterates are close from a local minimum of (1), and study its stability. Concretely, let $X_* \in \mathcal{O}_p$ such that $\psi(X_*) = 0$. We consider a small perturbation of X_* as $X = (I_p + A + S)X_*$, where $S \in \text{Sym}_p$ and $A \in \text{Skew}_p$ are small matrices.

Proposition 9 (First order expansion of Λ). *At the first order in (A, S) , we have $\Lambda((I_p + A + S)X_*) = \mathcal{J}(A, S)X_*$, with $\mathcal{J}(A, S) \triangleq \mathcal{H}_{X_*}(A) + \mathcal{H}_{X_*}^{\text{Sym}}(S) + \lambda S$, where \mathcal{H}_{X_*} is the Relative Hessian and $\mathcal{H}_{X_*}^{\text{Sym}}$ is a linear operator from Sym_p to Skew_p .*

The linear operator \mathcal{J} can be conveniently written in the basis $(\text{Skew}_p, \text{Sym}_p)$ where it is block-diagonal since for all $A \in \text{Skew}_p$, we have $\text{Sym}(\mathcal{J}(A, 0)) = 0$. The operator is written in this basis

$$\mathcal{J} = \begin{bmatrix} \mathcal{H}_{X_*} & \mathcal{H}_{X_*}^{\text{Sym}} \\ 0 & \lambda Id \end{bmatrix}.$$

As a consequence, the eigenvalues of \mathcal{J} are the eigenvalues of \mathcal{H}_{X_*} and λ : $\text{Sp}(\mathcal{J}) = \text{Sp}(\mathcal{H}_{X_*}) \cup \{\lambda\}$. This implies local convergence of the landing flow.

Proposition 10 (Local convergence, landing flow). *Assume that \mathcal{H}_{X_*} has positive eigenvalues, and let μ_{\min} the smallest one. Then, for any $\delta > 0$, there exists $\epsilon > 0$ such that if $\|X_0 - X_*\| \leq \epsilon$, the landing flow starting from X_0 verifies $\|X(t) - X_*\| = O(\exp(-(\min(\mu_{\min}, \lambda) + \delta)t))$.*

Proof. First, it is easily seen that X_* is an asymptotically stable point for the flow (see e.g. (Boyce et al., 2017, Theorem 9.3.2)). The convergence speed is then obtained with classical manipulations (for instance (Chicone, 2006, Corollary 4.23)). \square

Therefore, if $\lambda \geq \mu_{\min}$, we get the same local convergence speed for the landing flow and the Riemannian gradient flow. We obtain a similar result in the discrete case, using a Lipschitz assumption.

Proposition 11 (Local convergence, landing algorithm). *Assume that \mathcal{H}_{X_*} has positive eigenvalues, and let μ_{\min} the smallest one. Assume that Λ is L -Lipschitz. Then for any $\delta > 0$ there exists $\epsilon > 0$ such that if $\|X_0 - X_*\| \leq \epsilon$, the landing algorithm starting from X_0 with constant step $\eta \leq \frac{1}{L}$ verifies $\|X_k - X_*\| = O\left(\left(1 - \frac{\min(\mu_{\min}, \lambda)}{L} + \delta\right)^k\right)$.*

Proof. We first show that, starting close enough from X_* , the sequence X_k converges to X_* . A study of the difference between X_k and the iterates corresponding to the linear equation $X_{k+1} = X_k - \eta \mathcal{J}(X_k - X_*)$ then shows that both sequences have the same convergence speed. \square

Once again, when $\lambda \geq \mu_{\min}$, we get the same rate as Riemannian gradient descent (Zhang & Sra, 2016).

Global convergence results are beyond the scope of this paper. The study of the gradient flow on the manifold is in itself a difficult problem, and global convergence proofs usually require strong hypothesis like geodesic convexity of f (Zhang & Sra, 2016). In the case of \mathcal{O}_p , geodesic convexity is impossible to achieve since \mathcal{O}_p is not geodesically convex: geodesics are not uniquely defined.

Hyper-parameter trade-off. The hyper-parameter λ plays a key role in the convergence results. Proposition 11 suggests that λ should be greater than μ_{\min} . This constant is usually impossible to compute. This is mitigated by Proposition 6: if λ is high, we have $\eta^* \propto \lambda^{-1}$, and the safe interval becomes small, hindering the convergence speed of the algorithm when we are far from the solution. In the experiments, we take $\lambda = 1$, which in practice gives satisfying results.

3.4. A landing field for other manifolds ?

The landing field can in principle be extended to any (sub-)manifold \mathcal{M} of \mathbb{R}^d . Indeed, one can derive a field $G(x)$ and a potential $\mathcal{N}(x)$ such that when $x \in \mathcal{M}$, $G(x) = \text{Grad } f(x)$, such that $\nabla \mathcal{N}(x)$ is 0 if and only if $x \in \mathcal{M}$, and such that $G(x)$ and $\nabla \mathcal{N}(x)$ are always orthogonal. These properties are sufficient to obtain Proposition 4. However, these maps might not be tractable, while on \mathcal{O}_p their expressions are simple and cheap to compute. We describe two other classes of manifold on which one can also easily define a landing method.

Sphere manifold The sphere is $\mathcal{S} = \{x \in \mathbb{R}^d \mid \|x\| = 1\}$. We can define the “distance” as $\mathcal{N}(X) = \frac{1}{4}(\|x\|^2 - 1)^2$, and $G(x) = \nabla f(x) - \frac{\langle \nabla f(x), x \rangle}{\|x\|^2} x$. The landing field is then $\Lambda(x) = \nabla f(x) - \frac{\langle \nabla f(x), x \rangle}{\|x\|^2} x + \lambda(\|x\|^2 - 1)x$. However, there is no computational advantage of using the corresponding landing algorithm, because there are some cheap retractions on the sphere (for instance, computing the orthogonal projection only requires a scalar product).

Stiefel manifold The Stiefel manifold $\mathcal{S}_{n,p}$ is the set of *rectangular* matrices $X \in \mathbb{R}^{n \times p}$ with $n > p$ such that $X^\top X = I_p$. The Riemannian gradient of f is once again given by the

formula $\text{Grad } f(X) = \psi(X)X$, with $\psi(X) = \text{Skew}(\nabla f(X)X^\top)$. Here, $\psi(X)$ is a large $p \times p$ matrix. The distance function becomes $\mathcal{N}(X) = \|X^\top X - I_p\|^2$, and the landing field can then be defined as $\Lambda(X) = \psi(X)X + \lambda \nabla \mathcal{N}(X)$. We obtain the equivalent of Proposition 4 and Proposition 5: the points such that $\Lambda(X) = 0$ are exactly those for which $X \in \mathcal{S}_{n,p}$ and $\text{Grad } f(X) = 0$, and we get a similar orthogonalization property of the flow. We finish by stressing that some “fast” retractions are available for $\mathcal{S}_{n,p}$ when p is much smaller than n : Cayley retraction can be computed by inverting a small $2p \times 2p$ matrix. This trick using the Sherman-Morrison-Woodbury formula is presented in (Wen & Yin, 2013). In this setting, the landing flow might not be faster than this retraction.

3.5. Numerical errors

An advantage of our method is that it is robust to numerical errors. Indeed, if it converges, the landing flow goes to a point X such that $\|\Lambda(X)\|^2 \leq \delta_{\text{num}}$, where δ_{num} is a small constant that depends on the floating point precision. Since $\psi(X)X$ and $(XX^\top - I_p)X$ are orthogonal, we conclude that $\|XX^\top - I_p\|^2 \leq \delta_{\text{num}}$: at the limit, the landing algorithm makes an orthogonalization error of the order of the floating point precision. This is observed in practice.

On the contrary, consider for instance the exponential retraction. Starting from $X_0 \in \mathcal{O}_p$, it iterates $X_k = \exp(A_k)X_{k-1}$, where A_k is a skew-symmetric matrix. For simplicity, assume that $X_0 = I_p$. The iterate X_k can be compactly rewritten as $X_k = \prod_{i=1}^k \exp(A_i)$. Since A_k is skew-symmetric, all the $\exp(A_i)$ are orthogonal, so we indeed have $X_k \in \mathcal{O}_p$. But numerical computation of the matrix exponential comes with some numerical error, which means that $\exp(A_i)$ is not perfectly orthogonal in practice. To model the deviation to orthogonality, we write $\exp(A_i) = U_i + E_i$, where $U_i \in \mathcal{O}_p$, and E_i is a matrix of small norm. We let $P_i = U_i \times \dots \times U_1$. A first order expansion then gives $X_k \simeq P_k + P_k \sum_{i=1}^k P_i^\top E_i P_i$: the orthogonalization error increases with the number of iterations k . The same reasoning applies to Cayley retraction.

To conclude, the landing algorithm, while it is a non-feasible method, gives a solution that is more orthogonal than methods using the exponential or the Cayley retraction.

4. Experiments

We conclude by showcasing the usefulness of the landing algorithm on an array of optimization problems. The deep learning experiments are run on a single Tesla V100 GPU with Pytorch (Paszke et al., 2019), while the other experiments are run on a small laptop CPU and Numpy (Harris et al., 2020). The code for the landing flow as a Pytorch `Optimizer` and to reproduce the experiments is released at <https://github.com/pierreablin/landing>. In all experiments, we use the safe rule for the step-size described in Proposition 6, with $\varepsilon = 0.5$, and set $\lambda = 1$.

4.1. Experiments on orthogonal procrustes

We begin by a classical optimization problem. In the following, we let A, B two $p \times n$ matrices, and define the Procrustes cost function as $f(X) = \|XA - B\|^2$ where $X \in \mathcal{O}_p$.

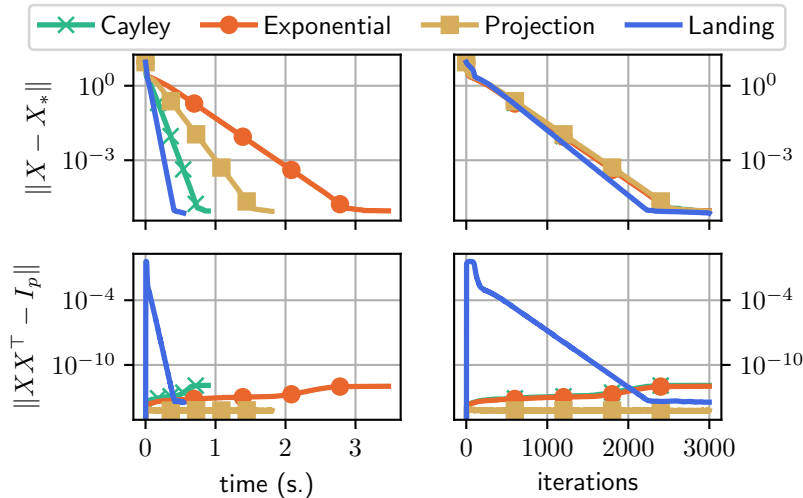


Figure 3: Gradient descent on the orthogonal procrustes problem using different retraction methods and the landing algorithm. Top: distance to the optimum. Bottom: distance to the orthogonal manifold. Left: w.r.t. time. Right: w.r.t. iterations.

We set $p = n = 40$. We generate A and B two random matrices with i.i.d. normal entries. We apply the different algorithms with a fixed step-size $\eta = 0.1$. We record the distance to the solution X_* , and the orthogonalization error $\|XX^\top - I_p\|$. Figure 3 displays the results.

Looking at the distance to the optimum, all methods are similar in term of iterations. Looking closer at the trajectories, we observe that they are actually almost identical. But since one iteration of the landing algorithm is cheaper, we get an overall faster method. Looking at the distance to the manifold, the landing algorithm starts by moving away from the manifold, but in the end lands on the manifold. The exponential and Cayley retractions suffer from numerical errors, and end up being further from the manifold than the landing algorithm.

4.2. Orthogonalization property

The goal of this experiment is to showcase the orthogonalization property of the landing algorithm. We set the dimension as $p = 100$. We start from $X_0 = I_p$, and add a small error $X = X_0 + E$, where E has i.i.d. entries of law $\mathcal{N}(0, \sigma^2)$, with $\sigma = 10^{-4}$. Therefore, X is close to, but not perfectly in \mathcal{O}_p . Then, we generate a random ‘gradient’, that is a random matrix $A \in \text{Skew}_p$ of i.i.d. entries where $A_{ij} \simeq \mathcal{N}(0, \gamma^2)$ for $i > j$, where γ controls the scale of the ‘gradient’ A . Setting $\gamma = 0$ emulates a solved optimization problem, where the gradient is 0. Setting γ small emulates an optimization problem closed from being solved, and γ high emulates an optimization problem far from being solved.

For the different retractions and the landing algorithm, we perform a step in the direction of A , with step-size $\eta = .3$. For the landing algorithm, we set $\lambda = 1$. In other words, we take the output as $X_{out} = \tilde{\mathcal{R}}(X, \eta A)$ for the retraction algorithms, and $X_{out} = X - \eta (AX + XX^\top - I_p)$ for the landing algorithm. We then record the

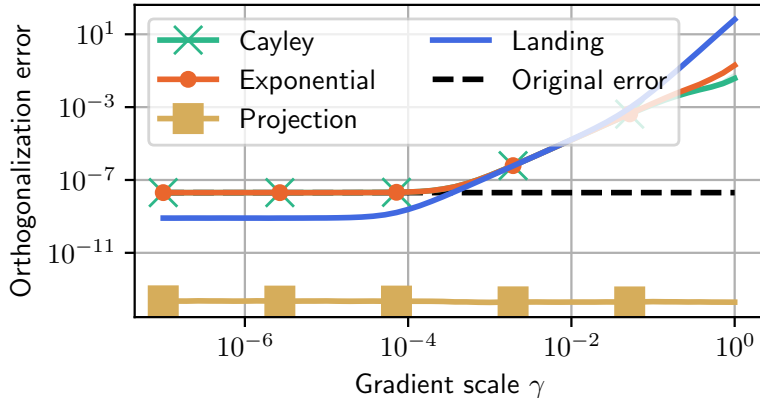


Figure 4: Orthogonality error after one step of each algorithm, starting from a matrix that is close to, but not on \mathcal{O}_p .

orthogonality error of the output, $\|X_{out}X_{out}^\top - I_p\|$.

For each γ , we repeat the experiment 50 times with different random seeds. Figure 4 shows the average orthogonality error of the different algorithms as a function of the gradient scale γ . As expected, the projection retraction yields a very small orthogonalization error, which only corresponds to the numerical errors. The exponential and Cayley retraction do not have this correcting effect, hence the orthogonalization error stays the same if the gradient scale is small. However, when the gradient scale gets large enough, these methods start to have greater numerical errors, and actually increase the orthogonalization error.

Finally, the landing algorithm has a hybrid behavior. When the gradient scale is small, it acts mainly as a cheap projection algorithm, which means that the orthogonalization error decreases. Here, one iteration reduces the error by a factor 10, so after a few iterations the algorithm would reach numerical precision. Then, as the gradient scale increases, we observe the same behavior as the other algorithms: the error increases. Finally, when the gradient scale is large enough, since the algorithm does not stay on the manifold, we see that the error gets bigger than all the other algorithms.

This illustrates a “self-correcting” behavior of the landing algorithm: unlike the exponential and Cayley retractions, it can decrease the orthogonalization error.

4.3. Applications in deep learning

We now turn to applications in deep learning, where the function f involves a neural network. Here, all computations are performed using Pytorch and a GPU. In this part, we discard the projection retraction, which is orders of magnitude more costly to compute than other retractions on a GPU (see Figure 2).

Fully connected network We begin by considering a fully connected neural network of depth L that maps the input $x_0 \in \mathbb{R}^p$ to the output $x_L \in \mathbb{R}^p$ following the recursion $x_{n+1} = \tanh(W_n x_n + b_n)$, where $W_n \in \mathbb{R}^{p \times p}$ are the weight matrices and $b_n \in \mathbb{R}^p$

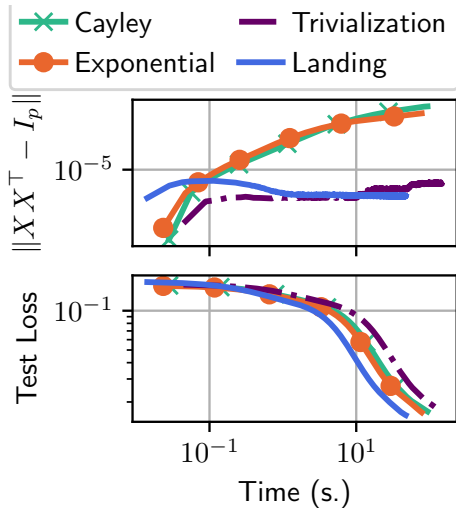


Figure 5: Training a fully connected neural network with orthogonal weights. We use the different methods mentioned in the text, and the proposed landing algorithm. Top: average orthogonalization error of all weights as training progresses. Bottom: test loss.

are the biases. We impose an orthogonal constraint on the weight matrices: $W_n \in \mathcal{O}_p$ for $n = 0 \dots L$. We denote $\Phi_\theta(x)$ the output of the network with input $x \in \mathbb{R}^p$ and parameters $\theta = (W_1, b_1, \dots, W_L, b_L)$. In this experiment, we consider a *distillation* problem Hinton et al. (2015): we generate a set of parameters θ^* that gives the target *teacher* network Φ_{θ^*} . Then, starting from a random parameter initialization, we try to learn the mapping Φ_{θ^*} with a *student* network with parameters θ , by minimizing the loss $\mathcal{L}(\theta) = \sum_{q=1}^Q \|\Phi_\theta(x^q) - \Phi_{\theta^*}(x^q)\|^2$, where the x^q are the training examples, drawn i.i.d. from a Gaussian $\mathcal{N}(0, 1)$ distribution. We consider the optimization of the orthogonal weights W_1, \dots, W_L with different methods. We use stochastic Riemannian gradient descent using the exponential or Cayley retraction or the landing flow. We also consider a trivialization method (Lezcano Casado, 2019), where each matrix is parametrized as $W_i = \exp(A_i)$ with $A_i \in \text{Skew}_p$, and the optimization is carried over A_i . We use matrices of size $p = 100$, with a depth $L = 10$. The learning rate is $\eta = 0.1$, and the batch size is 256. The orthogonalization error and test error are displayed in Figure 5. The landing flow is the fastest method. It also leads to smaller orthogonalization error than the other retraction methods, because it does not suffer from accumulation of numerical errors (see subsection 3.5). We also get to an error close to the one predicted in Equation (10). Interestingly, it has also a lower orthogonalization error than the trivialization method. After inspection, we found that the matrices A_i learned by the trivialization method were very large, which might explain the high numerical error.

LeNet on MNIST Finally, we train a LeNet5 (LeCun et al., 1998) for classification on the MNIST dataset. The network has 3 convolutional layers, and we impose an orthogonal constraint on the square kernel matrices. We take a batch size of 8, and a learning rate of $\eta = 0.005$. We compare the same algorithms as before; we could not get a satisfying accuracy with the trivialization method. Figure 6 displays the results of our experiment. The landing flow is 50% faster than the exponential retraction, and yields matrices that are more orthogonal.

Discussion We have presented a novel method to replace retraction-based algorithms on the orthogonal manifold. Our method is faster than retractions, it is therefore interesting

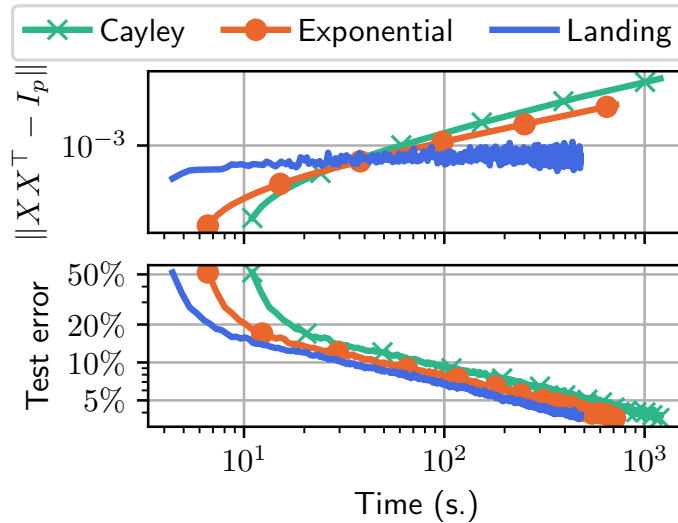


Figure 6: Training a LeNet5 with orthogonal weights on MNIST. Top: orthogonalization error. Bottom: Test accuracy.

to use in settings where computing a retraction is the computational bottleneck. It is also useful when one needs a solution that is accurately orthogonal, since it suffers less from numerical errors than widely used retractions. Future research directions include the development of second-order methods in this framework, and a thorough extension to the Stiefel manifold.

Acknowledgement

This work was supported by the French government under management of Agence Nationale de la Recherche as part of the “Investissements d’avenir” program, references ANR19-P3IA-0001 (PRAIRIE 3IA Institute).

References

- Ablin, P., Cardoso, J.-F., and Gramfort, A. Faster ICA under orthogonal constraint. In *2018 IEEE International Conference on Acoustics, Speech and Signal Processing (ICASSP)*, pp. 4464–4468. IEEE, 2018.
- Absil, P.-A. and Malick, J. Projection-like retractions on matrix manifolds. *SIAM Journal on Optimization*, 22(1):135–158, 2012.
- Absil, P.-A., Baker, C. G., and Gallivan, K. A. Trust-region methods on Riemannian manifolds. *Foundations of Computational Mathematics*, 7(3):303–330, 2007.
- Absil, P.-A., Mahony, R., and Sepulchre, R. *Optimization algorithms on matrix manifolds*. Princeton University Press, 2009.

- Absil, P.-A., Mahony, R., and Trunpf, J. An extrinsic look at the Riemannian Hessian. In *International Conference on Geometric Science of Information*, pp. 361–368. Springer, 2013.
- Arjovsky, M., Shah, A., and Bengio, Y. Unitary evolution recurrent neural networks. In *International Conference on Machine Learning*, pp. 1120–1128, 2016.
- Balashov, M., Polyak, B., and Tremba, A. Gradient projection and conditional gradient methods for constrained nonconvex minimization. *Numerical Functional Analysis and Optimization*, 41(7):822–849, 2020.
- Bansal, N., Chen, X., and Wang, Z. Can we gain more from orthogonality regularizations in training deep networks? 31:4261–4271, 2018. URL <https://proceedings.neurips.cc/paper/2018/file/bf424cb7b0dea050a42b9739eb261a3a-Paper.pdf>.
- Bonnabel, S. Stochastic gradient descent on Riemannian manifolds. *IEEE Transactions on Automatic Control*, 58(9):2217–2229, 2013.
- Boyce, W. E., DiPrima, R. C., and Meade, D. B. *Elementary differential equations*. John Wiley & Sons, 2017.
- Cardoso, J.-F. and Laheld, B. H. Equivariant adaptive source separation. *IEEE Transactions on signal processing*, 44(12):3017–3030, 1996.
- Chicone, C. *Ordinary differential equations with applications*, volume 34. Springer Science & Business Media, 2006.
- Comon, P. Independent component analysis, a new concept? *Signal processing*, 36(3):287–314, 1994.
- Edelman, A., Arias, T. A., and Smith, S. T. The geometry of algorithms with orthogonality constraints. *SIAM journal on Matrix Analysis and Applications*, 20(2):303–353, 1998.
- Harris, C. R., Millman, K. J., van der Walt, S. J., Gommers, R., Virtanen, P., Cournapeau, D., Wieser, E., Taylor, J., Berg, S., Smith, N. J., et al. Array programming with numpy. *Nature*, 585(7825):357–362, 2020.
- Hinton, G., Vinyals, O., and Dean, J. Distilling the knowledge in a neural network. *arXiv preprint arXiv:1503.02531*, 2015.
- Karimi, H., Nutini, J., and Schmidt, M. Linear convergence of gradient and proximal-gradient methods under the polyak-lojasiewicz condition. In *Joint European Conference on Machine Learning and Knowledge Discovery in Databases*, pp. 795–811. Springer, 2016.
- LeCun, Y., Bottou, L., Bengio, Y., and Haffner, P. Gradient-based learning applied to document recognition. *Proceedings of the IEEE*, 86(11):2278–2324, 1998.
- Lezcano Casado, M. Trivializations for gradient-based optimization on manifolds. *Advances in Neural Information Processing Systems*, 32:9157–9168, 2019.

- Nishimori, Y. Learning algorithm for independent component analysis by geodesic flows on orthogonal group. In *IJCNN'99. International Joint Conference on Neural Networks. Proceedings (Cat. No. 99CH36339)*, volume 2, pp. 933–938. IEEE, 1999.
- Oja, E. Simplified neuron model as a principal component analyzer. *Journal of mathematical biology*, 15(3):267–273, 1982.
- Paszke, A., Gross, S., Massa, F., Lerer, A., Bradbury, J., Chanan, G., Killeen, T., Lin, Z., Gimelshein, N., Antiga, L., et al. Pytorch: An imperative style, high-performance deep learning library. *arXiv preprint arXiv:1912.01703*, 2019.
- Qi, C., Gallivan, K. A., and Absil, P.-A. Riemannian BFGS algorithm with applications. In *Recent advances in optimization and its applications in engineering*, pp. 183–192. Springer, 2010.
- Rodríguez, P., Gonzalez, J., Cucurull, G., Gonfaus, J. M., and Roca, X. Regularizing cnns with locally constrained decorrelations. *arXiv preprint arXiv:1611.01967*, 2016.
- Schönemann, P. H. A generalized solution of the orthogonal procrustes problem. *Psychometrika*, 31(1):1–10, 1966.
- Tripuraneni, N., Flammarion, N., Bach, F., and Jordan, M. I. Averaging stochastic gradient descent on Riemannian manifolds. *arXiv preprint arXiv:1802.09128*, 2018.
- Wen, Z. and Yin, W. A feasible method for optimization with orthogonality constraints. *Mathematical Programming*, 142(1):397–434, 2013.
- Yan, W.-Y., Helmke, U., and Moore, J. B. Global analysis of Oja’s flow for neural networks. *IEEE Transactions on Neural Networks*, 5(5):674–683, 1994.
- Zhang, H. and Sra, S. First-order methods for geodesically convex optimization. In *Conference on Learning Theory*, pp. 1617–1638, 2016.
- Zhang, H. and Sra, S. Towards Riemannian accelerated gradient methods. *arXiv preprint arXiv:1806.02812*, 2018.

A. Proofs

A.1. Proof of Proposition 1

We recall the Euclidean Taylor expansion of f , where $\nabla f(X)$ is the gradient of f at X and H_X the Hessian of f at X :

$$f(X + E) = f(X) + \langle \nabla f(X), E \rangle + o(\|E\|), \quad (11)$$

$$\nabla f(X + E) = \nabla f(X) + H_X(E) + o(\|E\|). \quad (12)$$

The relative gradient $\psi(X)$ is such that

$$f(X + AX) = f(X) + \langle \psi(X), A \rangle + o(A).$$

Letting $E = AX$ in (11) gives, on the other hand

$$f(X + AX) = f(X) + \langle \nabla f(X), AX \rangle + o(A).$$

Identification of the first order term shows that for all $A \in \text{Skew}_p$, it holds

$$\langle \psi(X), A \rangle = \langle \nabla f(X), AX \rangle,$$

or by transposition:

$$\langle \psi(X) - \nabla f(X)X^\top, A \rangle = 0.$$

This scalar product cancels for all $A \in \text{Skew}_p$, so the matrix on the left has to be in the orthogonal of Skew_p , i.e. it is a symmetric matrix. In other words, its skew-symmetric part cancels. We therefore have

$$\text{Skew}(\psi(X) - \nabla f(X)X^\top) = 0,$$

and since $\psi(X)$ is skew-symmetric, we find

$$\psi(X) = \text{Skew}(\nabla f(X)X^\top).$$

For the relative Hessian, we have

$$\begin{aligned} \psi(X + AX) &= \text{Skew} \left(\nabla f(X + AX)(X + AX)^\top \right) \\ &= \text{Skew} \left((\nabla f(X) + H_X(AX))(X + AX)^\top \right) + o(A) \\ &= \text{Skew} \left(\nabla f(X)X^\top \right) + \text{Skew} \left(H_X(AX)X^\top \right) + \text{Skew} \left(\nabla f(X)X^\top A^\top \right) + o(A) \end{aligned}$$

By identification of the first order term, we find

$$\mathcal{H}_X(A) = \text{Skew} \left(H_X(AX)X^\top - \nabla f(X)X^\top A \right).$$

A.2. Proof of Proposition 2

The Riemannian gradient, $\text{Grad } f(X)$, and Hessian, $\text{Hess } f(X)$, are such that for $\xi \in \mathcal{T}_x$, it holds

$$f(\mathcal{R}(X, \xi)) = f(X) + \langle \text{Grad } f(X), \xi \rangle + \frac{1}{2} \langle \xi, \text{Hess } f(X)[\xi] \rangle + o(\|\xi\|^2),$$

where $\mathcal{R}(X, \xi)$ is the exponential retraction: $\mathcal{R}(X, \xi) = \exp(\xi X^\top)X$. We find using the same method as above:

$$\begin{aligned} \text{Grad } f(X) &= \text{Skew}(\nabla f(X)X^\top)X \\ \text{Hess } f(X)[\xi] &= \text{Skew}\left(H_X(\xi)X^\top - \text{Sym}(\nabla f(X)X^\top A)\right)X. \end{aligned}$$

This gives the expected identities.

A.3. Proof of Proposition 3

By contradiction, such polynomial must satisfy:

- Orthogonality: for all $X \in \mathcal{O}_p$ and $A \in \text{Skew}_p$, $P(X, A)P(X, A)^\top = I_p$.
- Retraction: for all $X \in \mathcal{O}_p$ and $A \in \text{Skew}_p$, $P(X, A) = X + AX + o(A)$.

The first equality shows that the polynomial PP^\top is a constant polynomial, it is therefore a polynomial of degree 0. Since the degree of PP^\top is greater than the degree of P , P must also be a constant polynomial. This contradicts the second equality.

A.4. Proof of Proposition 4

If $\Lambda(X) = 0$, since X is invertible, we have $\psi(X) + \lambda(XX^\top - I_p) = 0$. This is the sum of two matrices, one skew-symmetric, the other symmetric, which is zero. Therefore, both matrices are 0, and we deduce $\psi(X) = 0$ and $XX^\top = I_p$.

Conversely, if $X \in \mathcal{O}_p$ and $\psi(X) = 0$, we have $\Lambda(X) = 0$.

A.5. Proof of Proposition 5

By differentiation, denoting $n(t) = \mathcal{N}(X(t))$, we find

$$\dot{n}(t) = -\langle \Lambda(X(t)), \nabla \mathcal{N}(X(t)) \rangle \quad (13)$$

$$= -\langle \psi(X), (XX^\top - I)XX^\top \rangle - \lambda \|(XX^\top - I_p)X\|^2. \quad (14)$$

The first term cancels, since ψ is skew-symmetric and $(XX^\top - I)XX^\top$ is symmetric. Therefore, we obtain

$$\dot{n}(t) = -\lambda \|(X(t)X(t)^\top - I_p)X(t)\|^2 \quad (15)$$

Now, we would like to upper-bound this by a quantity involving only $n(t) = \|X(t)X(t)^\top - I_p\|^2$.

Dropping the time (t) for now, and letting $\Delta = XX^\top - I_p$, we find

$$\|(XX^\top - I_p)X\|^2 = \text{Tr}(\Delta XX^\top \Delta) \quad (16)$$

$$= \text{Tr}(\Delta(I_p + \Delta)\Delta) \quad (17)$$

$$= \|\Delta\|^2 + \text{Tr}(\Delta^3) \quad (18)$$

Next, we need to control $\text{Tr}(\Delta^3)$. Denoting $\lambda_1, \dots, \lambda_p$ the eigenvalues of Δ , we have $\text{Tr}(\Delta^3) = \sum_{i=1}^p \lambda_i^3$. This is lower bounded by $-\sum_{i=1}^p |\lambda_i|^3$, and then using the non-increasing property of ℓ_p norms, we have

$$\left(\sum_{i=1}^p |\lambda_i|^3 \right)^{\frac{1}{3}} \leq \left(\sum_{i=1}^p |\lambda_i|^2 \right)^{\frac{1}{2}},$$

and gathering all inequalities together, we have:

$$\text{Tr}(\Delta^3) = \sum_{i=1}^p \lambda_i^3 \geq -\sum_{i=1}^p |\lambda_i|^3 \geq -\left(\sum_{i=1}^p |\lambda_i|^2 \right)^{\frac{3}{2}} = -\|\Delta\|^3.$$

Finally, using $\mathcal{N}(X) = \|\Delta\|^2$, we find that Equation 18 gives the bound

$$\|(XX^\top - I_p)X\|^2 \geq \mathcal{N}(X) - \mathcal{N}(X)^{\frac{3}{2}}$$

We therefore obtain the differential inequation in Equation 15:

$$\dot{n}(t) \leq \lambda(n(t) - n(t)^{\frac{3}{2}}).$$

Dividing by the right hand side, we get

$$\frac{\dot{n}(t)}{n(t) - n(t)^{\frac{3}{2}}} \leq -\lambda.$$

And by integration, using the fact that $\gamma : x \mapsto \log(x) - 2 \log(1 - \sqrt{x})$ is a primitive of $x \mapsto \frac{1}{x - x^{\frac{3}{2}}}$, it holds:

$$\gamma(n(t)) - \gamma(N_0) \leq -\lambda t$$

which overall gives the bound

$$n(t) \leq \gamma^{-1}(-\lambda t + \gamma(N_0))$$

where the inverse of γ is $\gamma^{-1}(x) = \frac{1}{(\exp(-\frac{x}{2}) + 1)^2}$. We get:

$$n(t) \leq \frac{1}{(\exp(\frac{\lambda t - \gamma(N_0)}{2}) + 1)^2} \quad (19)$$

$$\leq \exp(-\lambda t) \frac{1}{(\exp(-\frac{\lambda t}{2}) + \exp(-\frac{\gamma(N_0)}{2}))} \quad (20)$$

The fraction on the right is then upper-bounded by $\exp(\frac{\gamma(N_0)}{2}) = \frac{N_0}{\sqrt{1 - N_0^2}}$, which gives the advertised result.

A.6. Proof of Proposition 6

Let $X \in \mathbb{R}^{p \times p}$, and define $\Delta = XX^\top - I_p$ and $A = \psi(X)$. The landing algorithm maps X to $\tilde{X} = (I_p - \eta(A + \lambda\Delta))X$. Defining $\tilde{\Delta} = \tilde{X}\tilde{X}^\top - I_p$, we find

$$\tilde{\Delta} = (I_p - \eta(A + \lambda\Delta))(\Delta + I_p)(I_p - \eta(-A + \lambda\Delta)) - I_p \quad (21)$$

$$= (1 - 2\eta\lambda)\Delta + (\eta - \eta^2\lambda)[A, \Delta] - (2\eta\lambda - \eta^2\lambda^2)\Delta^2 - \eta^2A^2 + \eta^2\lambda^2\Delta^3 + \lambda\eta^2[A, \Delta^2] - \eta^2A\Delta A, \quad (22)$$

where $[A, \Delta] = A\Delta - \Delta A$ is the Lie bracket.

Using the sub-multiplicativity of the norm, and the triangular inequality, denoting $a = \|A\|$ and $d = \|\Delta\|$, we get

$$\tilde{d} \leq (1 - 2\eta\lambda)d + 2(\eta - \eta^2\lambda)ad + (2\eta\lambda - \eta^2\lambda^2)d^2 + \eta^2a^2 + \eta^2\lambda^2d^3 + 2\lambda\eta^2ad^2 + \eta^2a^2d \quad (23)$$

$$\leq (1 - 2\eta\lambda)d + 2\eta ad + 2\eta\lambda d^2 + \eta^2a^2 + \eta^2\lambda^2d^3 + 2\lambda\eta^2ad^2 + \eta^2a^2d \quad (24)$$

Reordering terms in ascending powers of η , we find $\tilde{d} \leq d - \alpha\eta + \beta\eta^2$ with

$$\alpha = 2\lambda d - 2ad - 2\lambda d^2$$

$$\beta = a^2 + \lambda^2d^3 + 2\lambda ad^2 + a^2d > 0$$

Therefore, we find that when $\eta \leq \eta^*(\alpha, \beta) = \frac{\alpha + \sqrt{\alpha^2 + 4\beta(\varepsilon - d)}}{2\beta}$, we have $\tilde{d} \leq \varepsilon$.

A.7. Proof of Proposition 7

The proof of this result relies in the inequality (24), which is rewritten using indices as

$$d_{k+1} \leq (1 - 2\eta\lambda)d_k + 2\eta a_k d_k + 2\eta\lambda d_k^2 + \eta^2 a_k^2 + \eta^2\lambda^2 d_k^3 + 2\lambda\eta^2 a_k d_k^2 + \eta^2 a_k^2 d_k.$$

We let $v > 0$. By assumption, a_k goes to 0. Hence, for k large enough, $a_k \leq v$ which gives

$$d_{k+1} \leq (1 - 2\eta\lambda)d_k + 2\eta v d_k + 2\eta\lambda d_k^2 + \eta^2 v^2 + \eta^2\lambda^2 d_k^3 + 2\lambda\eta^2 v d_k^2 + \eta^2 v^2 d_k.$$

Using $d_k \leq \varepsilon$, we find

$$d_{k+1} \leq \kappa d_k + \eta^2 v^2, \quad (25)$$

where $\kappa = 1 - 2\eta\lambda + 2\eta v + 2\eta\lambda\varepsilon + \eta^2\lambda^2\varepsilon^2 + 2\lambda\eta^2 v\varepsilon + \eta^2 v^2$. Then, since v can be chosen arbitrarily small, and $\varepsilon < 1$, we can take v such that $\kappa < 1$. Then, unrolling Equation 25 gives

$$d_k \leq \kappa^k \left(d_0 - \frac{1}{1 - \kappa} \eta^2 v^2 \right) + \frac{1}{1 - \kappa} \eta^2 v^2$$

Since this holds for any v , it shows that $d_k \rightarrow 0$. We have therefore shown that if a_k goes to 0, then d_k also goes to 0.

Next, we focus on the specific rate of convergence. We once again consider $v > 0$. We take k large enough so that $d_k \leq v$ and $a_k \leq v$. We finally let $C > 0$ such that $a_k \leq C\omega^k$, and Equation 24 gives

$$d_{k+1} \leq (1 - 2\eta\lambda)d_k + 2\eta C\omega^k d_k + 2\eta\lambda v d_k + \eta^2 C^2 \omega^{2k} + \eta^2 \lambda^2 v^2 d_k + 2\lambda\eta^2 C\omega^k v d_k + \eta^2 v C^2 \omega^{2k}.$$

Collecting terms together:

$$d_{k+1} \leq \gamma_0 d_k + \gamma_1 \omega^k d_k + \gamma_2 \omega^{2k},$$

where $\gamma_0 = 1 - 2\eta\lambda + 2\eta\lambda v + \eta^2 \lambda^2 v^2$, $\gamma_1 = 2\eta + 2\lambda\eta^2 C v$ and $\gamma_2 = \eta^2 C^2 + \eta^2 v C^2$. Next, using $d_k \leq 1$, the middle term is majorized by $\gamma_1 \omega^k$. The last term is majorized by $\gamma_2 \omega^k$, yielding

$$d_{k+1} \leq \gamma_0 d_k + \gamma_3 \omega^k,$$

where $\gamma_3 = \gamma_1 + \gamma_2$.

Unrolling the recursion gives

$$d_k \leq \gamma_0^k d_0 + \gamma_3 \sum_{i=1}^{k-1} \gamma_0^{k-i} \omega^i = \gamma_0^k d_0 + \frac{\gamma_3}{\gamma_0 - \omega} (\gamma_0^{k+1} - \omega^{k+1})$$

which gives an upper-bound of the form

$$d_k \leq \alpha \gamma_0^k + \beta \omega^k$$

where α and β are constants. Since we can take ϵ arbitrarily small (and therefore, γ_0 arbitrarily close to $1 - 2\eta\lambda$), we get the advertised result.

A.8. Proof of Proposition 8

The proof idea is similar to the previous one. Since we also have $a_k \rightarrow 0$, we already know that d_k goes to 0. Next, we let C such that $a_k \leq Ck^\alpha$. We take k large enough so that $d_k \leq v$ and $a_k \leq v$. Equation 24 gives

$$d_{k+1} \leq (1 - 2\eta\lambda)d_k + 2\eta C k^\alpha d_k + 2\eta\lambda v d_k + \eta^2 C^2 k^{2\alpha} + \eta^2 \lambda^2 v^2 d_k + 2\lambda\eta^2 k^\alpha v d_k + \eta^2 v C k^{2\alpha}.$$

Using $k^{2\alpha} \leq k^\alpha$ and $d_k \leq 1$, we get the bound

$$d_{k+1} \leq \beta_0 d_k + \beta_1 k^\alpha$$

where $\beta_0 = 1 - 2\eta\lambda + 2\eta\lambda v + \eta^2 \lambda^2 v^2$ and $\beta_1 = 2\eta C + \eta^2 C^2 + 2\lambda\eta^2 v + \eta^2 v C$.

Unrolling the recursion gives

$$d_k \leq \beta_0^k d_0 + \beta_1 \sum_{i=1}^k \beta_0^{k-i} i^\alpha$$

We then use the equivalence

$$\sum_{i=1}^k \beta_0^{-i} i^\alpha \sim \beta_0^{-k} k^\alpha$$

to conclude that the second term is equivalent to k^α . Since the first term is smaller than k^α , this concludes the proof.

A.9. Proof of Proposition 9

We recall that

$$\Lambda(X) = \left(\psi(X) + \lambda(XX^\top - I_p) \right) X$$

Letting $X = (I_p + S + A)X_*$, we have at the first order

$$\psi(X) = \mathcal{H}_{X_*}(A) + \mathcal{H}_*^{Sym}(S)$$

and

$$XX^\top - I_p = S$$

which overall gives

$$\Lambda(X) = \mathcal{J}(A, S)X_*$$

with $\mathcal{J}(A, S) = \mathcal{H}_{X_*}(A) + \mathcal{H}_*^{Sym}(S) + \lambda S$.

A.10. Proof of Proposition 10

First, it is easily seen that since \mathcal{J} is invertible, then the system $\dot{X} = -\Lambda(X)$ is an “almost linear” system (Boyce et al., 2017, Ch.9.3), and the eigenvalues of \mathcal{J} are all non-negative and real, which shows that X_* is asymptotically stable: therefore, there exists $\delta > 0$ such that the flow, initialized from any X such that $\|X - X_*\| \leq \delta$, converges to X_* . Classical manipulations then give us the advertised convergence speed.¹

A.11. Proof of Proposition 11

The landing flow with step $\eta = \frac{1}{L}$ iterates $X_{k+1} = \Phi(X_k)$ with $\Phi(X) = X - \frac{1}{L}\Lambda(X)$. The Jacobian of this map is $Id - \frac{1}{L}\mathcal{J}(\Lambda)(X)$, where $\mathcal{J}(\Lambda)$ is the Jacobian of Λ . The eigenvalues of this map are the $1 - \frac{\mu}{L}$, where μ spans the eigenvalues of $\mathcal{J}(\Lambda)(X)$.

Since the eigenvalue of $\mathcal{J}(\Lambda)(X)$ are all real positive at X^* , there is a neighborhood of X^* such that in that neighborhood, the eigenvalues of $\mathcal{J}(\Lambda)(X)$ are close to real positive: for $\delta > 0$, there is a neighborhood of X^* such that for μ an eigenvalue of $\mathcal{J}(\Lambda)(X)$, we have $Re(\mu) > \min(\mu_{min}, \lambda)$ and $|Im(\mu)| \leq \delta$. Further, thanks to the Lipschitz assumption, we have $|\mu| \leq L$.

As a consequence, the eigenvalues of Φ , in this neighborhood, are of modulus squared:

¹See for instance corollary 4.23 of “Chicone, Carmen. Ordinary differential equations with applications. Vol. 34. Springer Science & Business Media, 2006.”

$$|1 - \frac{\mu}{L}|^2 = (1 - \frac{\text{Re}(\mu)}{L})^2 + \eta^2 \text{Im}(\mu)^2 \quad (26)$$

$$\leq (1 - \frac{\min(\mu_{\min}, \lambda)}{L})^2 + \eta^2 \delta^2 \quad (27)$$

Hence, the iterative scheme $X_{k+1} = \Phi(X_k)$ converges at the speed $O((1 - \frac{\min(\mu_{\min}, \lambda)}{L})^k)$.

B. Experiments details

B.1. Distillation experiment

The network is a fully-connected multilayer perceptron of depth L that maps the input x_0 to the output x_L by the iteration $x_{n+1} = \sigma(W_{n+1}x_n + b_{n+1})$, where $W_n \in \mathcal{O}_p$ and $b_n \in \mathbb{R}^p$, and σ is the tanh function. We denote $\Phi_\theta(x)$ the output of the network with input $x \in \mathbb{R}^p$ and parameters $\theta = (W_1, b_1, \dots, W_L, b_L)$. We set $p = 100$, and $L = 10$. We choose a random set of parameters $\theta^* = (W_1^*, b_1^*, \dots, W_L^*, b_L^*)$ as the teacher network, and starting from a new random initialization, we try to approximate this network.

We let θ the new parameters, and minimize the loss

$$\mathbb{E}_{x \sim d} [\|\Phi_\theta(x) - \Phi_{\theta^*}(x)\|^2]$$

where the density d is $\mathcal{N}(0, 1)$.

This is done with stochastic gradient descent, using a retraction for orthogonal parameters. The learning rate is set to 0.1, and we perform 10000 iterations with a batch size of 256.

B.2. MNIST experiment

We consider a standard LeNet network defined in Pytorch by:

```
class LeNet5(nn.Module):
    def __init__(self, n_classes=10, triv=False):
        super(LeNet5, self).__init__()
        self.conv1 = nn.Conv2d(in_channels=1, out_channels=6, kernel_size=5, stride=1)
        self.nonlin = nn.Tanh()
        self.avg1 = nn.AvgPool2d(kernel_size=2)
        self.conv2 = nn.Conv2d(in_channels=6, out_channels=16, kernel_size=5, stride=1)
        self.avg2 = nn.AvgPool2d(kernel_size=2)
        self.conv3 = nn.Conv2d(in_channels=16, out_channels=120, kernel_size=4, stride=1)
        self.fc1 = nn.Linear(in_features=120, out_features=n_classes)

    def forward(self, x):
        x = self.conv1(x)
        x = self.nonlin(x)
        x = self.avg1(x)
        x = self.conv2(x)
```



```
x = self.nonlin(x)
x = self.avg2(x)
x = self.conv3(x)
x = self.nonlin(x)
x = torch.flatten(x, 1)
x = self.fc1(x)
return x
```

It therefore consists of three convolutional layers: the first one maps one channel to 6 with a kernel of size 5×5 , the second maps the 6 channels to 16 with a kernel size of 5×5 , and the last one maps the 16 channels to 120 channels with a kernel size of 4×4 . A last linear layer is used to obtain an output in dimension 10. The kernel are assumed to be orthogonal. We use SGD with a batch size of 8, and a learning rate of 0.001.